Finite Element Modelling of the Steady Rolling of a Radial Tyre with Detailed Tread Pattern

Mir Hamid Reza Ghoreishy

Iran Polymer and Petrochemical Institute, P.O. Box: 14965/115, Tehran, Iran

A B S T R A C T

The differences and reliabilities of numerical results obtained by tyre models with simple tread and detailed patterns of rubber blocks are studied. The patterned tyre model was generated by combination of two separately developed finite element models. The first model consisted of all tyre components except tread pattern by revolving the tyre cross-section about its symmetry axis. On the other hand, the geometries of the rubber blocks in tread pattern are separately created and discretized to generate finite element mesh of the tread part. These two tyre models were combined and a single 3D finite element model with tread pattern was generated. The incompatibility between the tread pattern mesh and the other parts was considered by using a mesh-tying algorithm. The results showed that if the main purpose of the tyre analysis is to study the global behaviour of the tyre such as determining the load-deflection curve or dynamic radius of the rolling tyre then, a finite element model with simply ribbed tread is sufficient. However, accurate computations of the stress and strain fields as well as contact pressure need a finite element model of the tyre with detailed tread pattern.

To whom correspondence to be addressed.
E-mail: M.H.R.Ghoreishy@ippi.ac.ir

INTRODUCTION

Despite the substantial works carried out in the field of simulation of car tyres, the finite element analysis of these intricate structures is mainly based on the development of models in which the complex shape of the tread patterns are replaced by a pattern-less or simply ribbed tread. On the other hand, due to the highly complex shape of the tread blocks, it is very difficult to develop valid and precise mesh with reasonable degree of refinement for all components of the tread pattern. Thus, very refined elements are required to achieve accurate results. Consequently, the computational cost and effort is normally higher compared to the cases in which the details of the tread pattern are ignored.

In addition, the structure of tyre without tread is nearly axisymmetric while the geometry of tread blocks are quite complex. Therefore, the finite element mesh generated for the body of tyre is not generally consistent with those created for the rubber blocks that exist on the tread surface. The basis of the knowledge of most tyre designers is based on the results obtained

from the finite element analysis of simple models.

To overcome this problem, some researchers tried to adopt a global/local approach in the early 1990s [1-3]. In this technique a global model with simply ribbed or pattern-less tyre is first analyzed and then a local model which only consists of a tread part in contact with ground is developed. The detail of the tread pattern is included in the latter model and a refined mesh is generally employed for the analysis. The results of the first model is used as the boundary condition and imposed on the second (local) model.

Although this approach directs tyre engineers to a straightforward and easy solution of the contact problem in patterned tyres, owing to ignorance of the interaction between states of the stress and strain in the tyre composite and tread elements, non-accurate solutions especially at contact zone are likely to be obtained.

In recent years, due to the advances in computational facilities (hardware and software) and also development of algorithms for combining incompatible meshes into a single model, investigators are trying to develop and apply full 3D model of patterned tyres to achieve more accurate and reliable results for different types of tyre analyses [4-7].

In this research work the steady state rolling behaviour of a steel-belted radial tyre was numerically investigated using two different finite element models. The first model consisted of a simply ribbed tread while in the second model the detail of the tread pattern was fully taken into consideration. In previous works, we have studied the rolling behaviour of this tyre by using a simply ribbed model [8,9]. Besides, a full 3D model with tread blocks was also developed to perform an analysis for this tyre under a vertical static load [6]. A thorough literature review on the finite element modelling of the rolling tyres was published in 2008 [10].

The aim of the present work was to carry out a comparative study between the results of the simulation of the tyre in rolling using two mentioned finite element models. This is in continuation with our previous efforts [6-9] on modelling of tyres. Particularly, since the tread blocks have significant influence in cornering, the effect of slip angle in this case was also taken into account. In order to verify the methodology and numerical algorithm used in this work, the

experimentally measured contact area, tyre deflection, and dynamic loaded radius of the tyre were compared with data calculated by both models. The results of the simulations are extensively explained and it is shown here that depending on the type of the parameter to be studied, it is essential to use a full 3D model with individual rubber blocks in tread.

FINITE ELEMENT MODEL

The selected tyre for this research is a 175/70R14 84T steel-belted radial tyre which was also utilized in preceding works [8-9]. The carcass of the tyre was constructed of a polyester body ply, a nylon cap ply and two steel belts, respectively. Three modules of ABASQUS code, namely, CAE, Standard, and Viewer were used, respectively, as the pre-processor, processor, and post-processor in this work. The basic assumption that was made in this work was to ignore viscoelasticity, as all material behaviours were assumed to be hyper-elastic (for rubbers) and linear elastic (for reinforcing cords).

Two 3D finite element models were developed. In the first model, the complex shape of the tread pattern was replaced by four simple ribs in circumferential direction. In order to generate this model, a 2D axisymmetric finite element mesh was first created in the (r,z) plane of the cylindrical coordinate system. Then a 3D model was generated by revolving 2D elements about their symmetry axis. Figure 1 shows
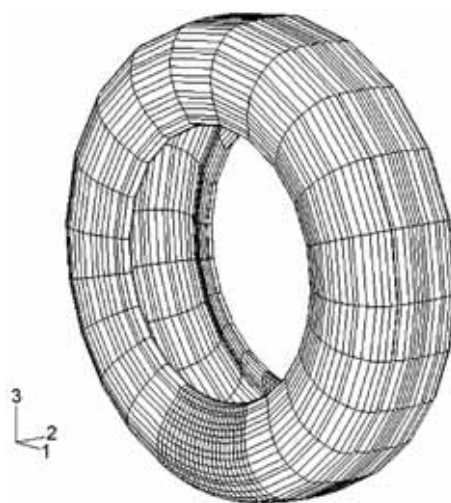

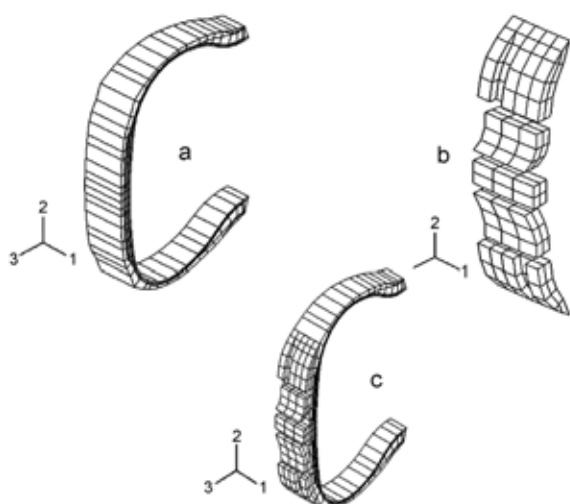**Figure 1.** Finite element mesh of the first model with simply ribbed tread.

Figure 2. Finite element meshes of the (a) symmetric part without tread pattern, (b) tread pattern and (c) symmetric part + tread pattern.

Figure 3. Finite element mesh of the full 3D model with tread blocks.

the finite element mesh of the first model which was also used in our previous works [8-9]. The total number of elements and nodes for this model were 12321 and 10402, respectively.

The development of the second model was, however, quite different from the first model. We first developed a 2D axisymmetric model of the tyre without tread part. This section was then revolved about its symmetry axis only for an angle of 5.625°, which is the rotational angle of a repeating unit of the tyre tread blocks. The geometry of the repeating section was then created in GEOSTAR software [11] and meshed using 3D brick elements. A uniform pitch for the geometry of the tread blocks was assumed in this work.

Figures 2a and 2b show the finite element meshes of the symmetric part (tyre without tread) and tread blocks, respectively. These two meshes are then assembled and a unique mesh is created as shown in Figure 2c. The total number of elements and nodes for this model are 414 and 787, respectively. Using the symmetric model generation algorithm implemented in ABAQUS, the single 3D sector of the model (Figure 2c) was revolved 64 times about tyre symmetry axis to create a full 3D finite element mesh of the tyre with detailed tread blocks located on its surface (Figure 3). The number of periodical repeating unit, 64, was derived from division of a full rotation angle (360°) by angle of initial sector (5.625°
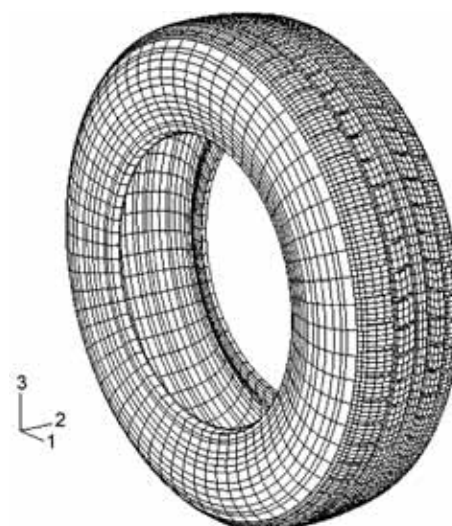
as described earlier). Total number of elements and nodes for the complete 3D model are 26497 and 32386, respectively. The key issue in generating such 3D finite element model is that the mesh configurations at interface between the tread and symmetric part of the tyre do not match correspondingly, and thus numerical difficulties in finding solutions at interfacial nodes are inevitable.

A tying algorithm which is implemented in ABAQUS [12] was used in this work. In this scheme, the displacements of each node on one surface (tyre body) are constrained such that they have the same values of the corresponding point on the other surface (tread elements). It should be noted that in the ABAQUS version 6.6, the theory of steady state rolling analysis is extended to take models that consist of periodic structures (such as a tyre with pattern) into account. Pneumatic tyre is a very complicated structure and it is not possible to adopt traditional methods such as the adaptive meshing which is used for determination of the optimum and converged finite element mesh. The process of the selection of an optimum finite element mesh in tyre analysis problem is a trade-off between maximum accuracy and the upper limit of the computational resources, e.g., CPU time and available amount of in-core and out-of-core memories. In order to find the best finite element mesh for this analysis we have checked several mesh configurations.

Table 1. Numerical values selected of material parameters in this simulation.

Material	Young's modulus (MPa)	Poisson's ratio	C_1* (MPa)	C_2* (MPa)
Nylon	3500	0.3	-	-
Polyester	9870	0.3	-	-
Steel cord	200,000	0.3	-	-
Rubber	-	-	0.41	0.083

(*) First and second parameters of the Mooney-Rivlin equation, $W = C_1 (I_1\text{-}3) + C_2 (I_2\text{-}3)$.

Our main strategy was based on the comparison made between the predicted data and experimental results and minimization of the equivalent Mises stress in a tread block mesh within 2% between two consecutive mesh configurations. Therefore, the selected mesh configurations (Figures 1-3) are found to exhibit the best compromise between the accuracy and computational cost and efforts while keeping the allowed error levels. In both models, the rubber components are modelled by the Mooney-Rivlin hyperelastic and the reinforcing fibres are represented by the linear elastic material models, respectively. The numerical values used for the material parameters in this simulation are presented in Table 1.

APPLIED LOADS AND BOUNDARY CONDITIONS

Each of the developed finite element model was used in four consecutive simulations. Similar procedures were adopted for both models. In the first step, an internal pressure of 0.248 MPa was applied inside the tyre surface to obtain the inflated shape of the tyre. In order to simulate the contact between the tyre tread and ground (footprint analysis) a pair of surfaces was defined. First, a rigid surface was defined that resembled the ground and considered as the master surface. This was an analytical (non-discretized) surface defined using spatial coordinates.

The second surface was, however, defined on the tread surface using elemental faces exposed to ground surface. Due to the large deformation and rotation that take place in tyre during loading, the finite sliding algorithm [12] was used at the contact solution strategy. In this approach, any arbitrary separation, sliding, and rotation of the nodal points on surface are taken into consideration. A point load (or concentrated load) of 4900 N (500 kg) corresponding to load index of 84 was applied on master (analytical rigid) surface. This has been carried out in two consecutive sections. In the first section, a displacement controlled approach was adopted in which the master surface was moved towards the tread surface by a small amount of displacement (say, 5 mm). Having generated an initial contact between ground and tyre tread, the final value of the load (500 kg) was applied via a force controlled approach and a deflected shape of the tyre under static vertical load was obtained. The friction between contact surface and tyre tread has been ignored (frictionless) in this stage.

The third step restarts from the results of the footprint analysis and a steady state rolling analysis was performed in an Arbitrary Lagrangin/Eulerian (ALE) framework implemented in the ABAQUS code [12]. A constant ground velocity of 60 km/h was assumed for the tyre. The tyre spinning velocity (rotational speed) was changed within a range from 54 rad/s to 60 rad/s to find the tyre free rolling condition and its dynamic loaded radius. The inertial effect and friction between tyre tread and ground were also considered in this step. A special formulation of the well-known Coulomb's law with a friction factor of 1.0 and slip tolerance of 0.005 was selected to model the frictional effect between tread surface and contact road.

The final stage was devoted to the inclusion of slip angle to model the rolling tyre in cornering condition. The tyre was analyzed using two slip angles of 1.5° and 3°, respectively. In all analyses the tyre rim was assumed to be constructed from very stiff materials so that the tyre was completely attached to the rim. Consequently, a fixed rim was selected as the boundary condition for both models. The other modelling parameters including material models, elastic constants, cord orientation, and spacing were selected to be similar in both models.

RESULTS AND DISCUSSION

All the finite element calculations were carried out

using ABAQUS/Standard version 6.6 [12] on a HP Compaq ML530 computer. The total run time for a typical simulation on this system including inflation, footprint, rolling, and cornering for the simply ribbed model and patterned tyre were 5445 s and 13077 s, respectively. It is clear that the time required to complete a simulation for the patterned tyre is more than twice the corresponding value for the simply ribbed model. To show the effect of the tread pattern on numerical results in tyre modelling problem, we have checked and compared the deformation of tyre, contact pressure and stress under various conditions using the mentioned models which are discussed in the following sections.

Figure 4 shows the load-deflection curve of the tyre under static vertical load. The deflection under the final load 4900 N for simply ribbed model and patterned tyre are 27.2 and 27.4 mm, respectively. The experimentally measured data are in the range of 26.5 to 28 mm for this tyre size. As it can be seen, both models predict almost identical results with negligible differences compared to experimental data. This means that the deflection behaviour under such load case has not been influenced by ignoring the tread pattern in the model. Referring to rolling analyses, the number of revolutions per km (R_k) was calculated. These values for the simply ribbed model and patterned tyre were 538 and 538.4, respectively. On the other hand, the measured value of this parameter for three commercial tyres was 546.3. Therefore, the change in computed values of this parameter is not
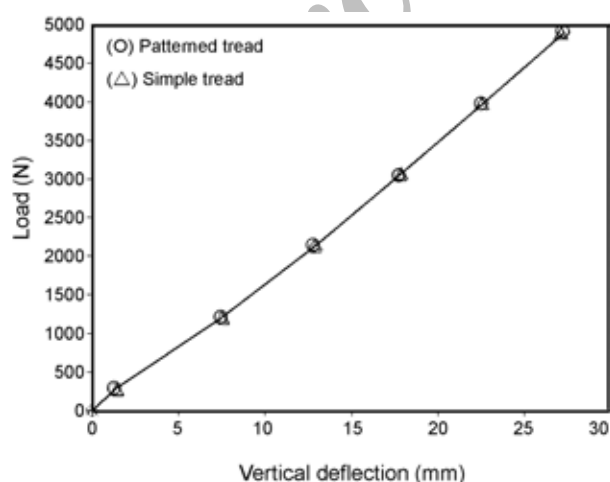
Table 2. Area of the contact patch with ground measured experimentally and computed by finite element models.

Area (mm^2)		
Experimentally measured	Predicted by simply ribbed model	Predicted by patterned model
16250	17764	16762

remarkable when the tread pattern is replaced by simple ribs.

It is also worth noting that owing to the inertial effect consideration, the calculated values of R_k in these simulations are slightly lower than the values reported in our previous work [8]. The contact area of the tyre predicted by two mentioned models was compared with experimentally measured data as recorded in Table 2. Although both models predicted the contact area of the tyre within a highly reasonable degree of accuracy which confirmed the correctness of the methodology used in this work, the predicted contact area by patterned tyre model is more precise than value computed by the simply ribbed model.

The distributions of contact pressures for both models under static vertical load and steady state rolling condition are represented in Figures 5a, 5b, 6a and 6b, respectively. The contact length and contact width refer to longitudinal and lateral directions, respectively. In all cases, the maximum contact pressure is located at shoulder zones. This phenomenon is already observed and reported [13].

However, considering the pressure distributions on rubber blocks in patterned tyre, the maximum pressure shifts from block centre under static load towards block edge in rolling state. This is because of inclusion of frictional effect in rolling state, which results in generation of a tangential resistance between rubber and ground and thus the location of maximum pressure translated to form a new force balance. In addition, due to the reduction of the net contact area in patterned tyre, the computed value of maximum contact pressure in this tyre is higher than the associated value in tyre with simply ribbed tread. Tread pattern also changes the symmetric distribution of the contact pressure along both 1st and 2nd axes.

This can be examined by comparing the pressure fields shown in Figures 5b and 6b. This is mainly due
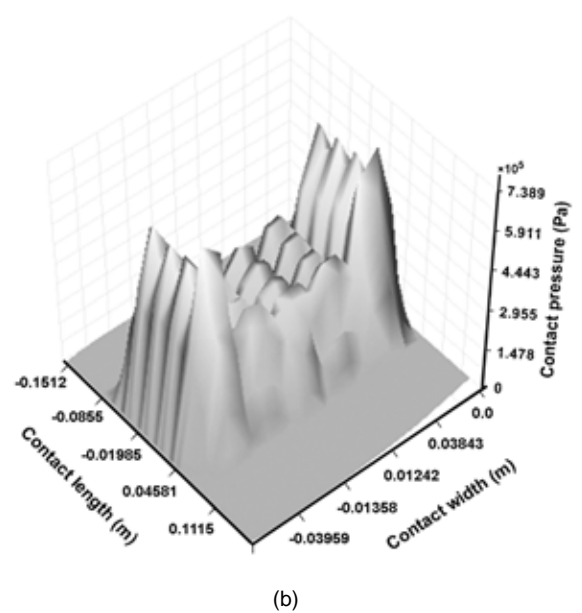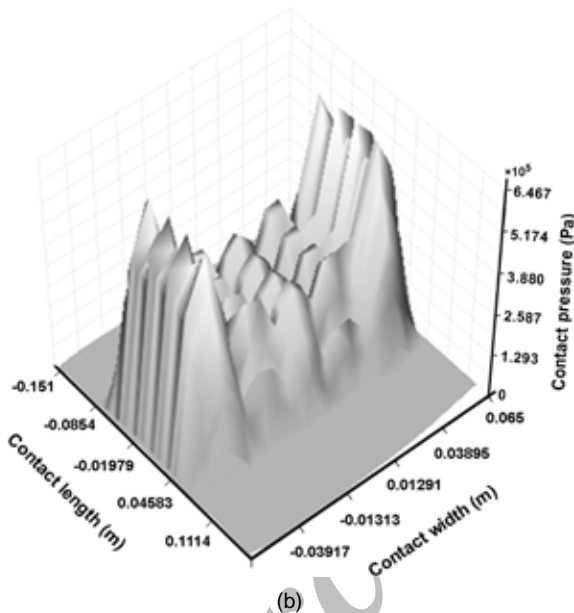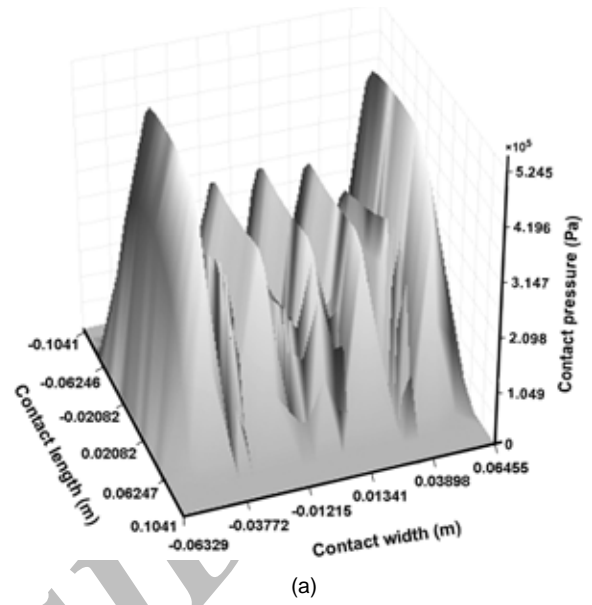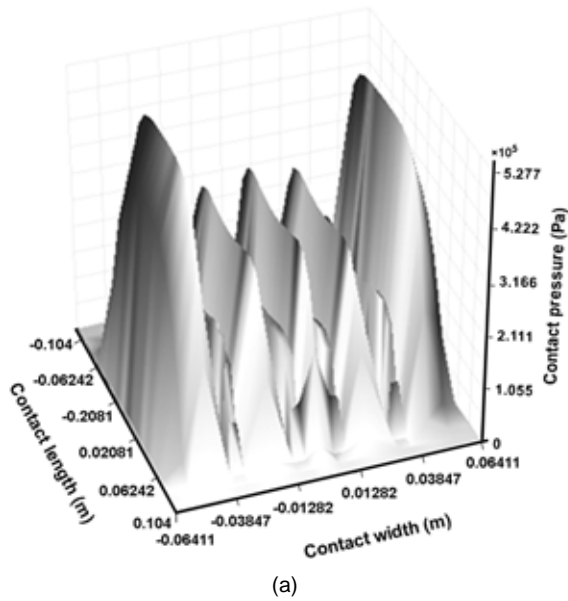

Figure 4. Load-deflection curve of the tyre for both models.
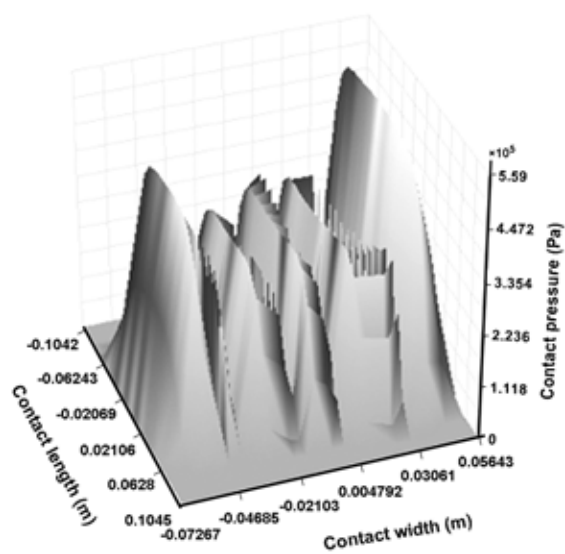
(a)

(b)

Figure 5. Distributions of contact pressure under static vertical load for: (a) simply ribbed and (b) patterned tyre models.
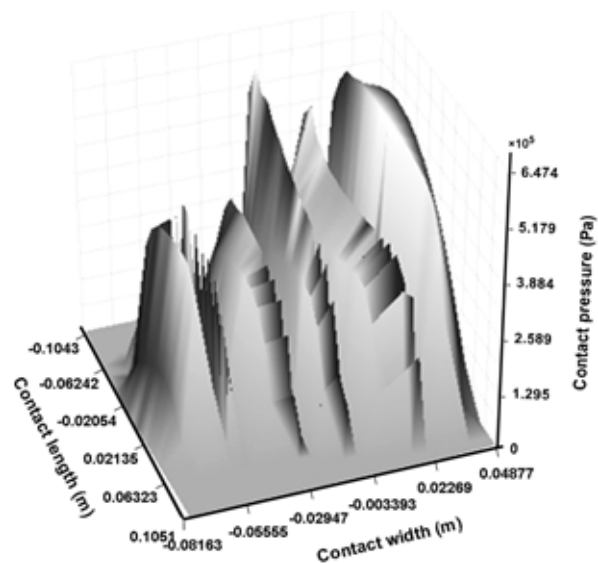

(a)

(b)

Figure 6. Distributions of contact pressure in free rolling state for: (a) simply ribbed and (b) patterned tyre models.

to the asymmetric geometries of the tread blocks and their locations on the tread surfaces. As it is mentioned earlier, tread pattern has strong influence on lateral behaviour of rolling tyres. This effect becomes more prominent when considering rolling tyre in cornering condition. Therefore, it would be interesting to study the effect of the slip angle in patterned and simply ribbed tyre models. When the slip angle (α) is set to 1.5º, as it is expected due to the generation of lateral (transverse) force, the contact

pressure becomes more non-homogeneous which can be seen in both models (Figures 7a and 7b). Similar distributions were obtained in both models in which the maximum pressure was located at shoulder zones. However, one can find out that the maximum pressure in simply ribbed model increases while it slightly decreases in patterned tyre. Increasing the slip angle to $\alpha = 3$º will give different results. In tyre model with simply ribbed tread only an increase in both non-homogeneity and maximum value of contact pressure was observed which was relatively

(a)
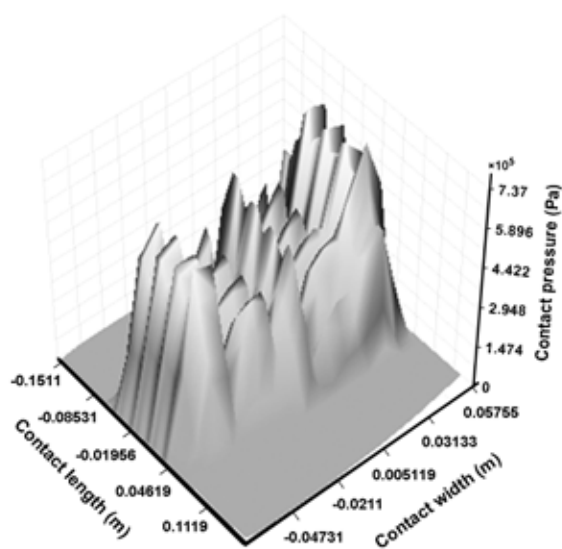
(b)

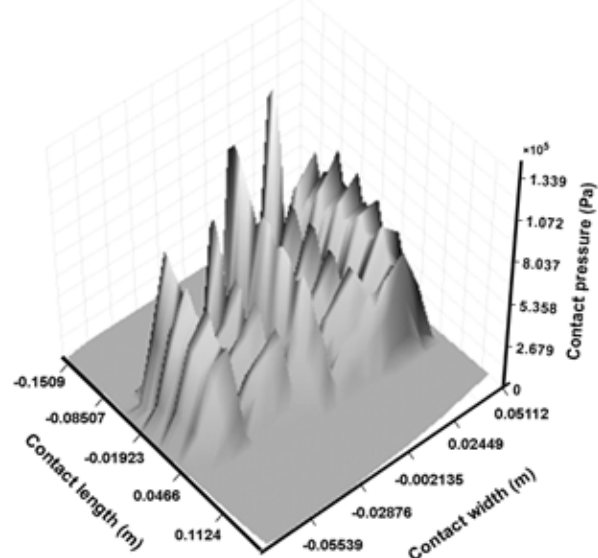**Figure 7.** Distributions of contact pressure in free rolling state for: (a) simply ribbed and (b) patterned tyre models with slip angle of 1.5º.

(a)

(b)

Figure 8. Distributions of contact pressure in free rolling state for: (a) simply ribbed and (b) patterned tyre models with slip angle of 3º.

predictable as shown in Figure 8a. In contrast, in patterned tyre the situation was rather different. The maximum contact pressure not only was no longer observed in shoulder zone and moved to the centre and trailing zone of the contact area but a more uniform pressure field was obtained compared to tyre model with simply ribbed tread (Figure 8b).

This could be justified based on the fact that in patterned tyres the rubber blocks are arranged on the tyre surface individually and thus the deformational

behaviour of each block is somewhat independent from other elements. In simply ribbed model, however, a unique and solid part is assumed for tread zone and therefore, any change in applied load and deformation would have direct influence on other parts. It other words the unsymmetrical nature of the tread pattern layout with respect to the longitudinal and lateral centre lines of the tyre plays the most important role in the difference between the predicted contact pressure at different slip angles. It should be

Table 3. Maximum values of stress components for simply ribbed model and patterned tyre at slip angles of 0º and 3º. Subscripts x, y and z are selected according to the SAE sign convention system (SAE J670e) [15] in which they refer to longitudinal, lateral and vertical directions, respectively.

Slip angle	$\alpha = 0^0$					
Stress component (MPa)	σ_{xx}	σ_{yy}	σ_{zz}	σ_{xy}	σ_{yx}	σ_{xz}
Simply ribbed model	174500	565.5	473.2	131.6	38.97	843.4
Patterned tyre	175200	575.7	1074	23.72	132.3	867.9
Slip angle	$\alpha = 3^0$					
Stress component (MPa)	σ_{xx}	σ_{yy}	σ_{zz}	σ_{xy}	σ_{yx}	σ_{xz}
Simply ribbed model	251900	735.5	746.3	154.5	60.23	1145
Patterned tyre	245600	901.9	2091	70.11	145.5	1290

also noted that ignoring the details of the tread pattern always gives unique results while for each pattern we may have a different distribution of the second order field variables such as the contact pressure of the present case [7].

Examining the stress field gives some valuable results especially at tyre composite sections under tread area (belts and cap ply). Some components of the stress field were changed significantly when the detail of the tread pattern is included in the model while some others remained relatively unchanged. Table 3 gives the maximum values of the six stress components under normal rolling (α=0) and slip angle of 3º. As an example, the difference in shear stress components σ_{xz}, and σ_{xx} between the patterned tyre and simply ribbed model are negligible. Moreover,

(a)

(b)

Figure 9. Distributions of shear stress component (σ_{xz}) in free rolling states of: (a) simply ribbed and (b) patterned tyre models.

S, S23
Multiple section points
(Avg: 75%)
+3.897×10⁴
+2.019×10⁴
+1.403×10³
-1.738×10⁴
-3.617×10⁴
-5.495×10⁴
-7.374×10⁴
-9.252×10⁴
-1.113×10⁵
-1.301×10⁵
-1.489×10⁵
-1.677×10⁵
-1.864×10⁵

(a)

S, S23
Multiple section points
(Avg: 75%)
+1.323×10⁵
+1.102×10⁵
+8.814×10⁴
+6.609×10⁴
+4.404×10⁴
+2.198×10⁴
-7.016×10¹
-2.212×10⁴
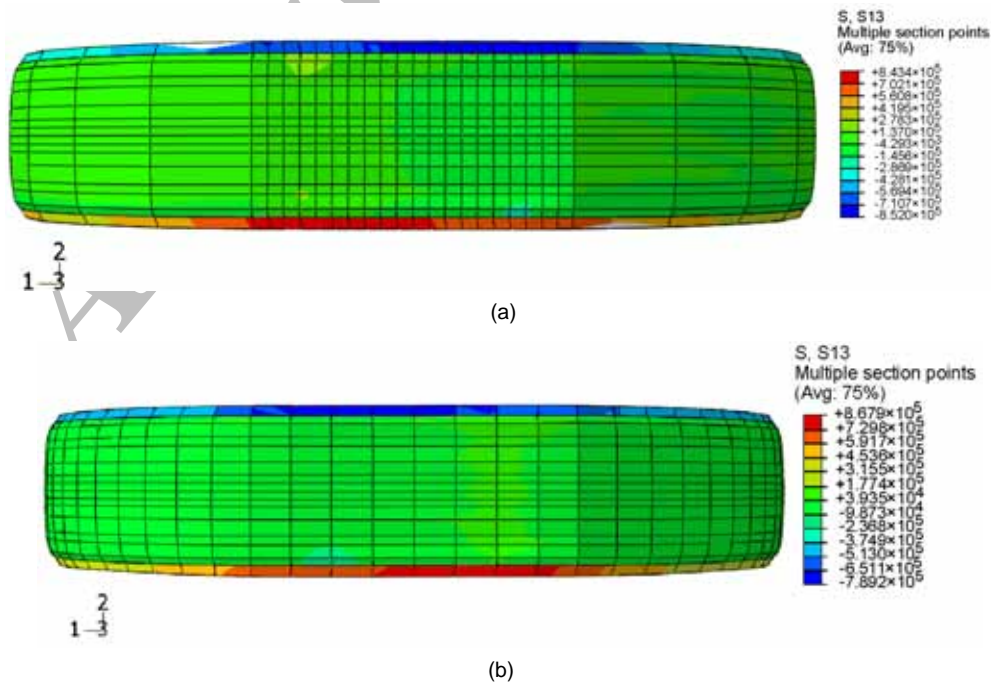-4.418×10⁴
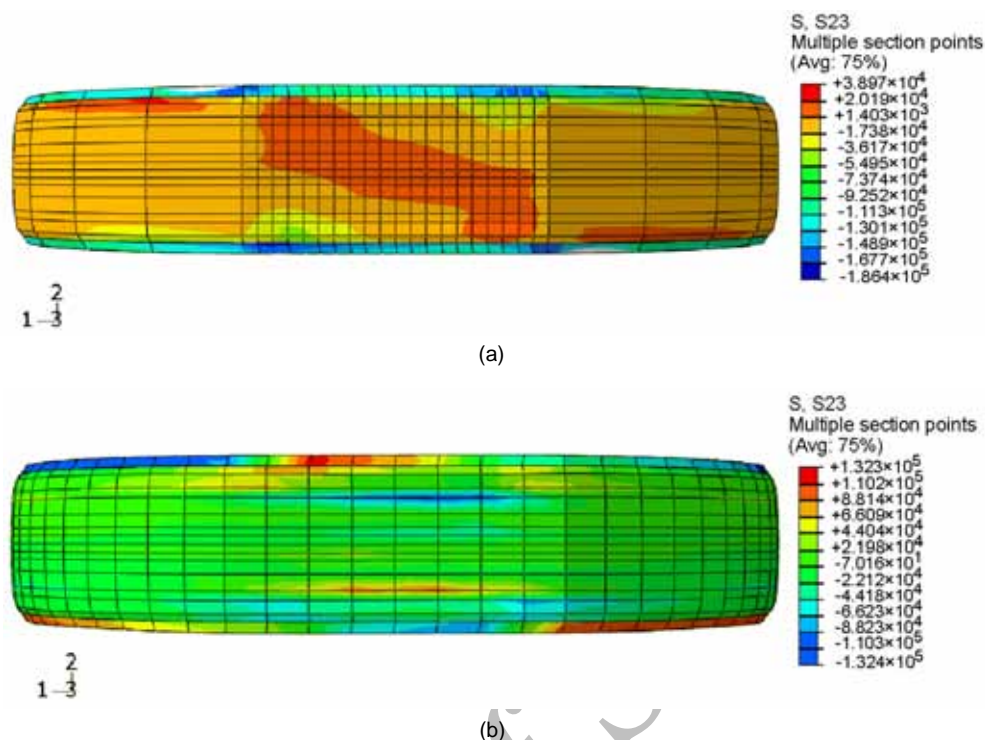-6.623×10⁴
-8.823×10⁴
-1.103×10⁵
-1.324×10⁵

(b)

Figure 10. Distributions of shear stress component (σ_{yz}) in free rolling states of: (a) simply ribbed and (b) patterned tyre models.

the longitudinal component (σ_{xx}) is much higher than the other components. This is due to the main tractive force that applies to the tyre in the first direction (x axis). However, this difference for shear component σ_{yz}, is very significant.

On the other hand, the difference becomes greater in cornering ($\alpha \neq 0$) which is due to the slip increasing lateral force. Considering the distributions of the stress components, it gives rise to similar results.

Figures 9a and 9b show the distributions of σ_{xz}, for both models at slip angle of zero. Also, Figures 10a and 10b represent the distribution of σ_{yz}, under the same conditions. As it can be seen, the distribution of σ_{xz}, for both models are nearly identical while major dissimilarities exist between the results of σ_{yz} in patterned tyre and simple ribbed model. The main justification for these results is that in patterned tyre, each rubber block behaves relatively independent from other parts while in ribbed tyre simply a unique tread part exists and thus the state of stress at each element is closely dependent on adjacent elements. The main effect of such difference in geometry is on the lateral behaviour of the tyre as it is discussed earlier. Therefore, those stress components that are

related to lateral direction (such as σ_{yz}) show noticeable changes in their variation and others remain rather unaffected. It may be also deduced here that the conventional global/local method, as stated previously [14], is not an appropriate scheme for the solution of contact problem in patterned tyre since it does not consider the state of stress and strain between the tread and elements of belts.

CONCLUSION

A numerical investigation was performed on the results of the finite element analysis of two tyre models. In the first model the tread pattern was replaced by a simply ribbed structure while the second model was comprised of details of the rubber blocks in a patterned tyre. Comparison of the results revealed that ignoring the details of the tread pattern has very minor effects on some lumped variables such as tyre deformation and dynamic loaded radius. However, more precise parameters especially those which have relations with contact zone (such as contact pressure) or have been related to lateral behaviour

are significantly affected when the tread patterns are included in the model. These phenomena become more prominent in cornering condition. In addition, depending on the components under study, the state of stress in interfacial zone between the tread and composite section in contact with tread (belts and cap ply) differs noticeably. Therefore, it can be concluded that if the prime purpose of the analysis is to study the global behaviour of the tyre, such as determining the load-deflection curve, then a finite element model with simply ribbed tread is sufficient, since in this case the high computational cost and effort of detailed models are avoided. On the other hand, obtaining accurate and reliable numerical results of the field variables such as contact pressure or state of stress (and strain) needs a refined mesh in conjunction with detailed modelling of tread pattern.

REFERENCES

1. Gall R, Tabaddor F, Robbins D, Majors P, Sheperd W, Johnson S, Some notes on the finite element analysis of tires, *Tire Sci Technol*, **23**, 175-188, 1995.

2. Seta E, Nakajima Y, Kamegawa T, Ogawa H, Hydroplaning analysis by FEM and FVM: effect of tire rolling and tire pattern on hydroplaning, *Tire Sci Technol*, **28**, 140-156, 2000.

3. Mundl R, Fischer M, Wajroch M, Lee S W, Simulation and validation of the ply steer residual aligning torque induced by the tyre tread pattern, *Veh Syst Dyn*, **43**, 434-443, 2000.

4. Cho JR, Kim KW, Yoo WS, Hong SI, Mesh generation considering detailed tread blocks for reliable 3D tire analysis, *Adv Eng Softw*, **35**, 105-113, 2004.

5. Cho JR, Kim KW, Jeon DH, Yoo WS, Transient dynamic response analysis of 3-D patterned tire rolling over cleat, *Eur J Mech A-Solid*, **24**, 519-531, 2005.

6. Ghoreishy MHR, Finite element analysis of a steel-belted radial tyre with tread pattern under contact load, *Iran Polym J*, **15**, 667-674, 2006.

7. Ghoreishy MHR, Malekzadeh M, Rahimi H, A parametric study on the steady state rolling behaviour of a steel-belted radial tyre, *Iran Polym J*, **16**, 539-548, 2007.

8. Ghoreishy MHR, Steady state rolling analysis of a radial tyre: comparison with experimental results, *Proc Inst Mech Engrs D J Auto Eng*, **220**, 713-721, 2006.

9. Ghoreishy MHR, Finite element analysis of a steady rolling tyre with slip angle: effect of belt angle, *Plast Rubber Compos: Macromol Eng*, **35**, 83-90, 2006.

10. Ghoreishy MHR, A state of the art review of the finite element modelling of rolling tyres, *Iran Polym J*, **17**, 571-597, 2008.

11. *COSMOS/M, Command reference, Version 1.75*, 1995.

12. *ABAQUS/Standard Theory Manual, Version 6.6*, 2006.

13. Browne A, Ludema KC, Clark SK, Contact between tyre and roadway. In: *Mechanics of Pneumatic Tires*, Clark SK (Ed), US Department of Transportation, Washington DC, USA, 249-363, 1981.

14. Gall R, Tabaddor F, Robbins D, Majors P, Sheperd W, Johnson S, Some notes on the finite element analysis of tires, *Tire Sci Technol*, **23**, 175-188, 1996.

15. Pacejka HB, *Tyre and Vehicle Dynamics*, 2nd ed, Butterworth-Heinemann, Oxford, Ch 1, 1-60, 2006.